Parachute Opening Shock Calculations with Experimentally Established Input Functions

H. G. Heinrich*
University of Minnesota, Minneapolis, Minn.
and
David P. Saari†
FluiDyne Engineering Corp., Minneapolis, Minn.

Parachute opening shock calculations with experimentally established area- and velocity-time functions are shown which, in combination with the momentum and continuity equations, yield force-time histories that satisfactorily agree in shape and force level with measured force-time diagrams. Two conjugate functions were found which approach uniqueness and provide satisfactory force-time histories of solid flat circular parachutes of 3-100 ft diameter, with loads of 0.5-5400 lb at snatch velocities between 50 and 360 fps.

Nomenclature

C_D = drag coefficient
C_DS = drag area
D = diameter, drag
d = inlet diameter
F = force
g = gravitational acceleration
L_s = suspension line length
m = mass
S = area
t = time
T = dimensionless time, t/t_f
u = outflow velocity due to cloth porosity
u/v = effective porosity
V = volume
v = velocity
v^*_{in} = fictitious net inflow velocity
W = weight
θ = trajectory angle
ρ = air density

Subscripts

a = apparent
f = filling
g = gravitational
i = included
in = inflow (inlet when used with S)
l = load
max = value at $T = 1.0$ when used with D_p, S_p, V
0 = initial (nominal when used with D and S)
p = parachute (projected when used with D and S)
s = snatch
T = total

I. Introduction

ATTEMPTS to analyze the parachute opening process and calculate the opening shock date back to 1927.[1] Since then a number of methods have been suggested, some of which are based primarily on analytical considerations.[2-4] However, it seems that these methods have not been developed to the point where results can be compared with wind-tunnel or field-test data.

Wolf[5] and McVey and Wolf[6] suggested a dynamic model consisting of point masses connected with elastic members and introduced a radial force coefficient related to a known drag coefficient. Utilizing the equations of axial and radial momentum gave force-time histories which agreed well with recorded data of tests with ribbon parachutes.

Among the earlier publications, O'Hara[7] is particularly appealing because it is relatively simple and provided, in earlier times, some reasonable predictions for maximum forces of solid cloth parachutes. O'Hara introduced the effect of cloth porosity, an assumption for the inflow velocity, and a model for the development of the parachute canopy during the inflation. O'Hara's model was a circular cylinder. The rate of increase of its radius, or the rate of inflation of the parachute, was then determined from the formulation of a continuity equation. The net inflow velocity, divided by the system's velocity, was assumed to decrease in proportion to the increasing radius and the canopy porosity. The equation of motion balanced the momentum change, assuming a horizontal trajectory and incorporating included and apparent mass, and the aerodynamic drag.

At the University of Minnesota, the O'Hara approach was developed further.[8,9] A geometric model consisting of a truncated cone, the sides of which were parallel to the suspension lines, and a hemispherical cap was introduced, and numerical values of effective porosity[10] and apparent mass[11,12] were used. As principal inputs to the equations of motion and continuity, it was assumed that the air inflow to the canopy and the canopy drag area varied linearly with time. This method gave very good approximations of the maximum opening forces of solid cloth parachutes.[9] However, the force-time histories of measured and calculated forces differed considerably.

The assumption that the inflow velocity and the drag area are linear with time is certainly arbitrary and probably causes the unrealistic calculated force-time diagrams. Also, these assumptions raise doubts as to the general applicability of this method. Therefore, in the following study, an attempt was made to extract time-related functions of the projected area and the inflow velocity of inflating parachutes from data of actual parachute tests.

It was postulated that a particular parachute type inflates approximately in the same manner, regardless of parachute

Presented as Paper 75-1382 at the AIAA 5th Aerodynamic Deceleration Systems Conference, Albuquerque, N. Mex., Nov. 17-19, 1975; submitted June 14, 1976; revision received Sept. 14, 1977.

Index category: Deceleration Systems.

*Professor. Fellow AIAA.
†Development Engineer. Member AIAA.

size and test conditions, and that an inspection of available data would yield characteristic functions of the inflow-time and area-time relationships. In turn, these functions, in combination with the equations of motion and continuity, govern the inflation process, and using the basic method described in Ref. 9, should give more satisfying results.

II. Equations Governing the Inflation

The parachute inflation begins when the process of snatch force development is completed. At this time, all suspension lines are stretched out behind the suspended load, and the parachute and load move with the same speed.[13] As the canopy inflates and the suspension lines assume certain angles to the centerline of the system, the center of mass of the parachute and included air mass moves forward, which is actually a relative velocity between load and canopy. However, this effect is opposed by the elongation of the highly elastic suspension lines. Consideration of both effects leads to a considerable complication of the system and its significance is uncertain. In most published theories, these effects are neglected, and it is assumed in the following that during inflation the parachute and the load travel with the same velocity.

In Ref. 14, it was shown that the equation of motion in the form of

$$d(m_T v)/dt = F_g - D_T \tag{1}$$

or more explicitly, and with D_p representing the drag of the parachute,

$$d[(m_l + m_p + m_i + m_a)v]/dt = (m_l + m_p)g\ \cos\theta - D_l - D_p$$

yielded good agreement between calculated force-time histories and force-time recordings from wind-tunnel tests. Of course, for the wind-tunnel application, Eq. (1) was modified, corresponding to a forced horizontal deployment. For calculations and comparisons with free-flight tests, Eq. (1) may be expanded to give

$$\frac{dv}{dt} = \left[(m_l + m_p)g\ \cos\theta - \frac{\rho v^2 (C_{D_l} S_l + C_{D_p} \pi D_p^2/4)}{2} - \frac{v}{t_f}\left(\frac{dm_i}{dt} + \frac{dm_a}{dt}\right)\right] m_T^{-1} \tag{2}$$

Introducing the centrifugal acceleration, one has, for a curved trajectory, the angular velocity

$$d\theta/dt = -(m_l + m_p)g\ \sin\theta/(m_T v) \tag{3}$$

Considering the flow through the inlet area and the hemispherical porous roof of the canopy, the filling time t_f follows from the continuity relationship

$$\frac{dV}{dt} = \pi \frac{d^2[v_{in} - 2u(D_p/d)^2]}{4} \tag{4}$$

The solution of Eqs. (2-4) provides then the opening force, since

$$F = m_l(g\ \cos\theta - dv/dt) \tag{5}$$

These equations include the functions of the parachute projected area, the included and apparent masses, and the inflow velocity. In order to solve them, velocity- and area-time functions are required. In the study reported herein, these functions were extracted from field and wind-tunnel test data.

III. Extraction of Input Functions

In view of the concept just outlined, an experimentally determined relationship of the projected canopy area S_p vs time, coupled with a geometric model, gives a volume-time history needed for the solution of the continuity equation. As a model for the intermediate shapes,[9,15] a family of truncated cones with hemispherical or ellipsoidal roofs may be used.

A method for extracting inflow functions from inflation test measurements was developed in Ref. 16 in the following manner. The continuity equation may be written as

$$dV/dt = (\pi d^2/4) v_{in}^* \tag{6}$$

where v_{in}^* is identical to the value in parentheses in Eq. (4). Physically, it is the actual inflow velocity minus an average velocity through the porous roof and the vent of the canopy. This term was called net inflow velocity and can be obtained from the rate of change of the canopy.

With $T = t/t_f$, the systems velocity v can be obtained from the impluse equation

$$v = v_0 - \left(\frac{t_f}{m_l}\right)\int_0^T F dT \tag{7}$$

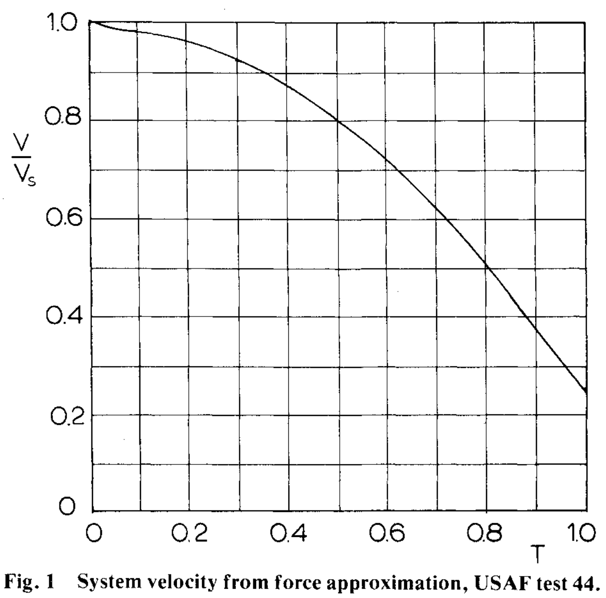

Fig. 1 System velocity from force approximation, USAF test 44.

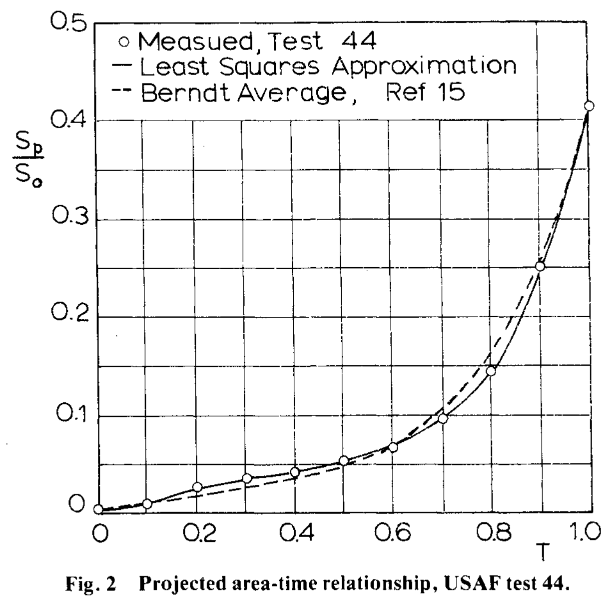

Fig. 2 Projected area-time relationship, USAF test 44.

Field test recordings showing force-time histories were obtained from the USAF Data Bank,[17] and the particular test identified as USAF No. 44 was selected for detailed analysis. In this test, a 28 ft flat circular man-carrying parachute, type C-9, was tested with a suspended weight of 439 lb, a snatch velocity of 225 fps, at an altitude of 6075 ft. The data indicated also a filling time of $t_f = 0.93$ s.

The force data were approximated by a least-squares polynomial function and the systems velocity calculated by means of Eq. (7) and Fig. 1. For the same test, the area-time function is shown in Fig. 2 together with an approximation suggested by Berndt.[15]

If the shape of the canopy during inflation is approximated by a truncated cone with a hemispherical cap, the proportions of which change with time, the volume of the canopy with suspension lines $L_s = D_0$ amounts to

$$\frac{V}{V_{\max}} = \frac{\pi^3}{8}\left\{ \frac{S_p}{S_0}\left[\left(\frac{3}{2} - \frac{\pi D_p}{4D_0}\right)^2 - \frac{S_p}{4S_0}\right]^{1/2} \times \frac{S_{\text{in}}}{S_0}\left(1 - \frac{S_{\text{in}}}{4S_0}\right)^{1/2} + \left(\frac{D_p}{D_0}\right)^3 \right\} \tag{8}$$

where

$$V_{\max} = \pi (D_{p_{\max}})^3 / 12 \tag{9}$$

and

$$S_{\text{in}} = \pi d^2 / 4 \tag{10}$$

The experimental area-time history (Fig. 2) combined with this assumed geometrical model, also provides the time history of the inlet area (Fig. 3). With Eq. (8) the area-time function also gives the time functions of volume and volume derivatives (Fig. 4).

By rewriting and expanding Eq. (6), one obtains the inflow velocity

$$v_{\text{in}}^* = \left(\frac{V_{\max}}{t_f S_0}\right)\left(\frac{S_0}{S_{\text{in}}}\right)\frac{\mathrm{d}(V/V_{\max})}{\mathrm{d}T} \tag{11}$$

and with the systems velocity v (Fig. 1), the dimensionless form

$$\frac{v_{\text{in}}^*}{v} = \frac{V_{\max}}{v_0 t_f S_0}\left(\frac{S_{\text{in}}}{S_0}\right)^{-1}\left(\frac{v}{v_0}\right)^{-1}\frac{\mathrm{d}(V/V_{\max})}{\mathrm{d}T} \tag{12}$$

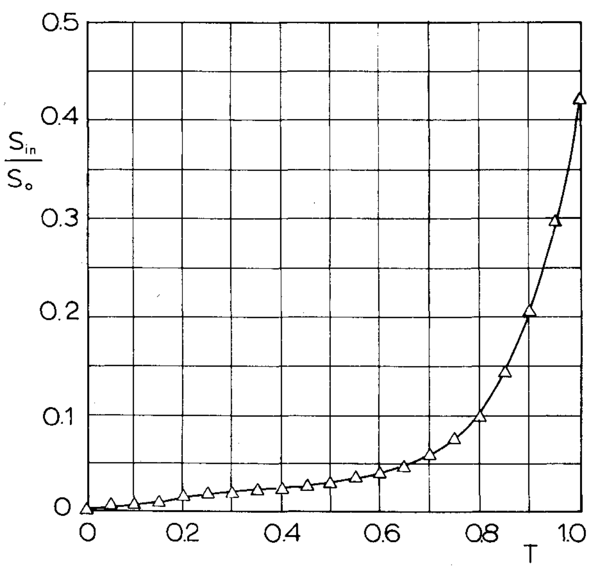

Fig. 3 Inlet area for test 44 based on projected area and geometrical model.

which is shown in Fig. 5. The dashed curve near $T = 0$ in Fig. 5 is drawn to comply with the initial physical conditions.

An area-time history, such as shown in Fig. 2, and an inflow function, as in Fig. 5, then provide the necessary information for a force calculation, as outlined in Sec. I.

IV. Review of the Terms of the Equation of Motion

If the filling time t_f is taken from Ref. 17, it encompasses, by definition, the time interval from the maximum snatch force until the projected area of the inflating canopy equals, for the first time, that of the canopy at steady descent.[13] However, this period also includes the time during which the canopy unfurls and some air streams into the canopy without being decelerated and developing into a stagnant mass. This initial phase may be relatively short; however, it is noticeable

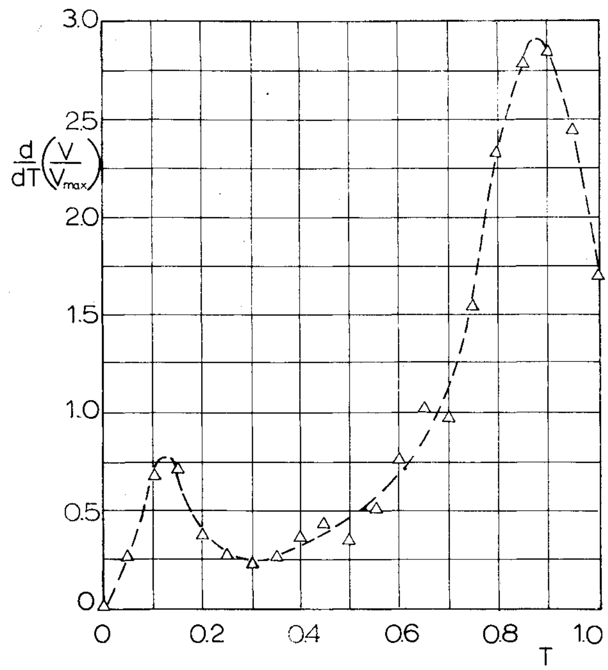

Fig. 4 Volume derivative for test 44 based on projected area and geometrical model.

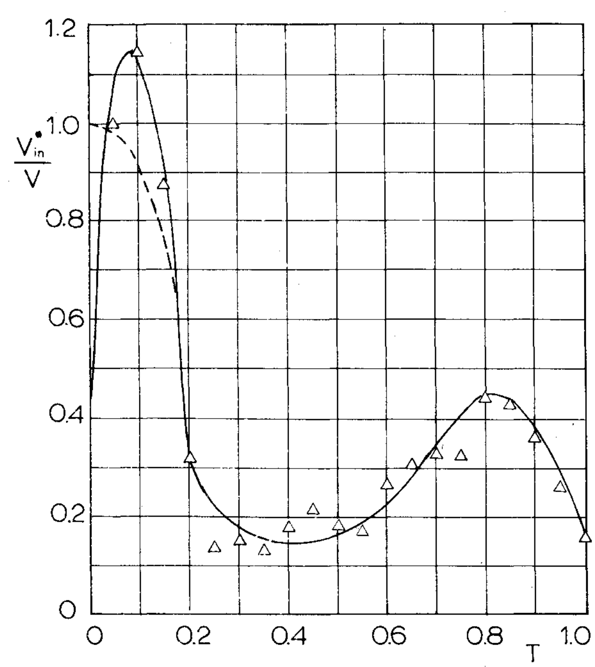

Fig. 5 Net inflow function for test 44.

in recordings, and this and other considerations require a general review of the terms to be introduced into the equations of motion [Eqs. (2) and (3)].

A. Filling Time

As explained, the filling time, in accordance with Ref. 13, includes a period in which events occur that are not really related to the dynamics of the inflating canopy.

Reviewing field test data, this period may be approximated as $0 \leq T \leq 0.15$, and this period is also approximately equal to the time that the air needs to move from the skirt to the apex of the stretched-out canopy, $t = D_0/2v_s$.

During this period, the canopy merely develops drag and Eqs. (2) and (3) are

$$dv/dt = g \cos\theta - (\rho v^2/2)[(C_D S)_l + (C_D S)_p](m_l + m_p)^{-1} \tag{13}$$

and

$$d\theta/dt = -(g \sin\theta)v^{-1} \tag{14}$$

with $(C_D S)_p$ representing the drag area of the stretched-out parachute.

B. Included and Apparent Mass

For a fully inflated parachute, it can be assumed that practically the entire canopy is filled with stagnant air moving with the parachute. Thus, the stagnant, or included, air mass at full inflation, is

$$m_i = \rho V_{\max} \tag{15}$$

However, during the filling process some air flows through the inlet area of the parachute and the entire canopy volume, as given by the geometrical model, is not filled with stagnant air, as assumed in Refs. 7 and 9. Actual shapes of an inflating parachute[15] suggest that primarily the air-filled dome is the portion of the canopy which is filled with stagnant air. This mass can be expressed as

$$m_i = \rho V_{\max}(D_p/D_{p_{\max}})^3 \tag{16}$$

The apparent mass is an expression of the hydrodynamic inertia of the external flowfield. The value of the apparent mass used in earlier studies[8,9] is based on measurements made on fully inflated parachutes,[11,12] modified by a coefficient which increases linearly from zero to unity as the parachute inflates. In this manner, a variation of the apparent mass is introduced, varying with the shape of the inflating canopy from a stretched-out cylinder to its steady-state condition. This variation was also used in the analysis of Ref. 14. In this form, the apparent mass amounts to

$$m_a = (0.25)T\pi\rho(D_p/2)^3 \tag{17}$$

where the factor 0.25 is obtained from Ref. 12 for solid cloth parachutes.

Relating the apparent mass to the included mass, as presented in Ref. 12 for fully inflated solid cloth parachutes, one obtains

$$m_a = (3/8)m_i \qquad (T=1) \tag{18}$$

Newer studies on the apparent mass were made by Ibrahim[18] and Klimas.[19] Saari[20] compared the results of Refs. 18 and 19 with the older study[12] and found relatively good agreement of the coefficients in the three studies as far as ribbon parachutes were concerned. Therefore, one may assume that the basic value of the coefficient 0.25 is a good approximation for actual cloth parachutes.

The modification with respect to time, T, in Eq. (17) is a postulation based on the linear variation of projected diameter, as used in Refs. 8 and 9. In order to retain a similar modification when using nonlinear inputs, the formulation for apparent mass was modified for this study to the form

$$m_a = (3/8)m_i(D_p/D_{p_{\max}})^2 \tag{19}$$

C. Shape Assumptions

Field tests[15,17] indicate that the projected area at full inflation amounts to $S_{p_{\max}} = 0.420 S_0$, while a geometrical model with a spherical cap amounts to $S_{p_{\max}} = 0.405 S_0$.

In order to avoid inconsistencies by using the USAF Data Bank data, the geometrical model was modified to include an ellipsoidal cap. This model has a maximum projected area $S_{p_{\max}} = 0.420 S_0$ at $T = 1$. The respective equations are

$$V = (\pi/12)\{0.661 D_p^3 + D_p^2[(L_s + D_0/2 - 0.665 D_p)^2 - D_p^2/4]^{1/2} - d^2(L_s^2 - d^2/4)^{1/2}\} \tag{20}$$

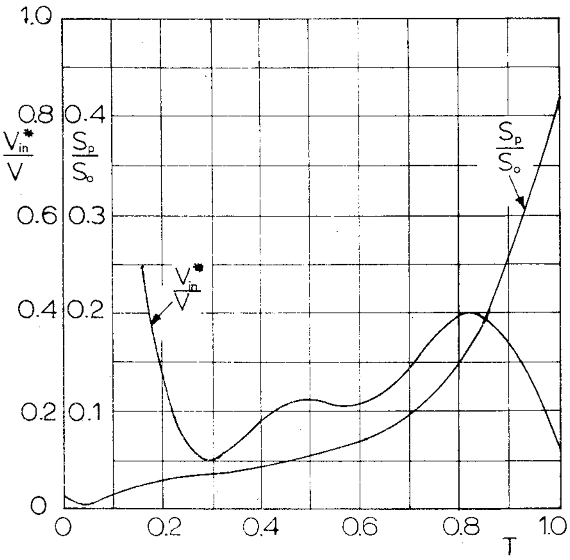

Fig. 6 Area and inflow function of test 44.

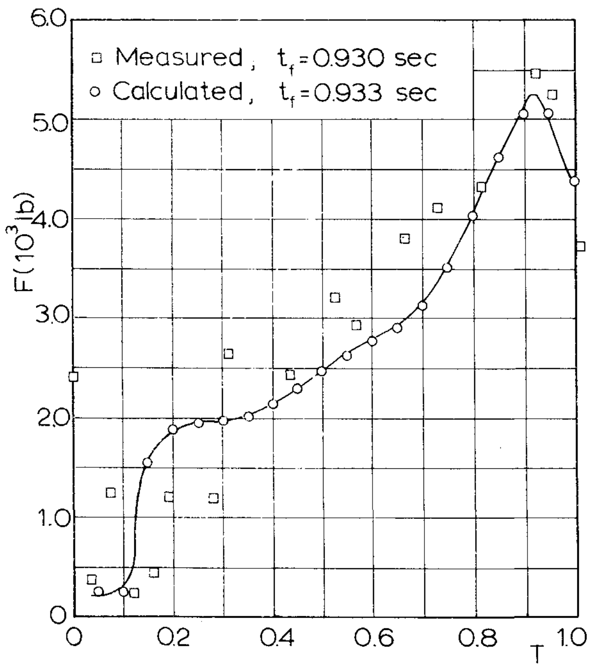

Fig. 7 Measured and calculated force-time histories for a 28-ft parachute, test 44, $v_s = 255$ fps, $W_l = 439$ lb.

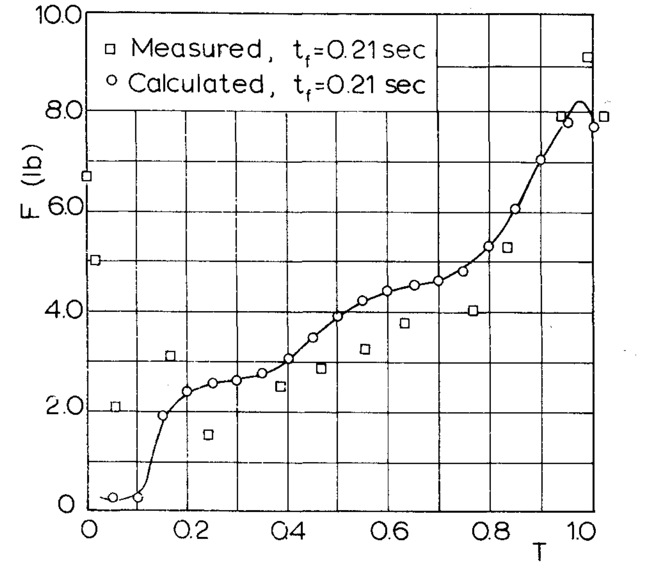

Fig. 8 Calculated and measured force-time histories for a 3-ft model parachute, $v_s = 70$ fps, $W_l = 0.5$ lb.

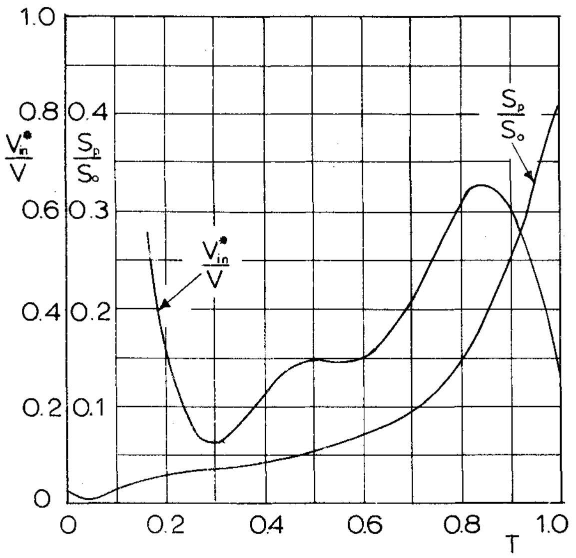

Fig. 9 "Unique" area and inflow functions

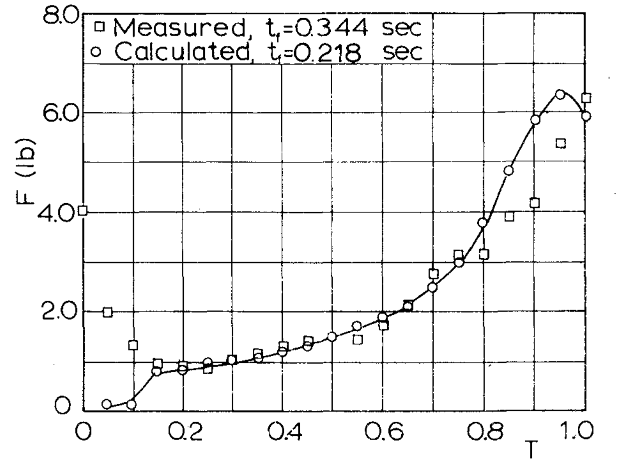

Fig. 10 Calculated and measured force-time histories for a 3-ft model parachute, $v_s = 50$ fps, $W_l = 0.5$ lb.

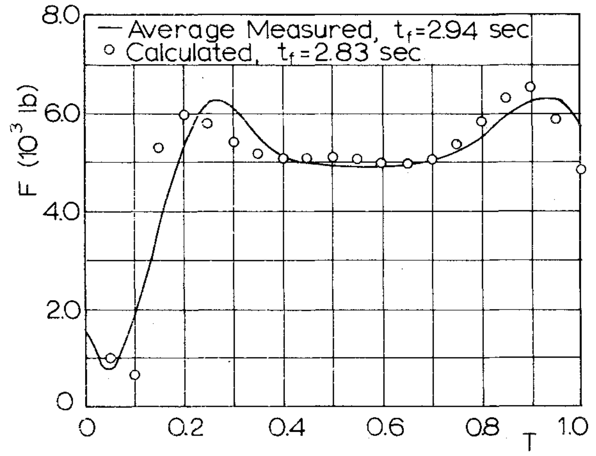

Fig. 11 Calculated and measured force-time histories for a 64-ft G-12 parachute, $v_s = 205$ fps, $W_l = 2200$ lb.

and

$$d = L_s D_p (L_s + D_0/2 - 0.665 D_p)^{-1} \tag{21}$$

D. Drag Coefficient

When related to the projected area of the geometrical model, the drag coefficient of a parachute during inflation is almost constant.[9] This result was found in wind-tunnel tests with models consisting of a wire frame, truncated cone with hemispherical cap, covered with a loosely fitted circular flat cloth canopy.

It is somewhat unconventional procedure to relate a drag coefficient to an area that changes with time; however, it is practical for this method of calculation since all other terms are also related to time. The approximation of a constant coefficient gave satisfactory results in Ref. 14. For this new study the approximation was reconsidered. However, sample calculations showed that a varying drag coefficient influenced the canopy drag force so little that this refinement did not justify the added complication. Therefore, in the following calculations, a constant drag coefficient of $C_{D_p} = 1.786$ was used, which is related to the instantaneous projected area of the parachute.

V. Test Cases and Unique Functions

The force- and area-time histories of USAF Test No. 44 were again analyzed, and the terms, as previously discussed, were incorporated. The related inflow and area functions are shown in Fig. 6. These functions, as well as those of the included and apparent masses, were introduced in the respective equations, and Fig. 7 shows data points of the measured and calculated force-time histories.

The same method of extracting time functions and utilizing the other established terms were then used to calculate the force-time history of a 3-ft model parachute which was inflated in a wind tunnel under finite mass condition at 70 fps with a suspended weight of 0.5 lb. The results are shown in Fig. 8.

In both cases, the agreement of the maximum forces is within the usual engineering accuracy and the force-time histories show the same general tendency.

Following these trials, a considerable number of cases were studied and calculated and measured data compared. In general, if for one particular test the area-time function and filling time as given in the USAF Data Bank were used, calculated and measured force-time histories matched each other as well as those cases shown in Figs. 7 and 8.

This agreement may be considered as proof of the validity of the method and the related approximations and assumptions.

The next objective was to find a pair of unique functions that would give satisfactory predictions when applied to parachute operations over a wide range of size, loading, and

Table 1 Calculated and measured maximum forces

Parachute, D_0, ft	Weight, W, lb	Snatch velocity, V_s, fps	Deviation, %
3	0.5	50	0
3	0.5	70	20
3	0.5	85	− 8
28	200	225	−17
28	200	306	−18
64	2200	205	1
64	2200	240	10
100	4550	184	2
100	5410	156	17

speed. For this purpose, the established area and velocity functions of the individual tests were applied to a number of cases. From these calculations emerged a pair of functions which approach uniqueness (Fig. 9). Using these functions, computed and measured force-time histories for a number of tests agreed to a degree similar to those shown in Figs. 10 and 11.

Numerical values of the time functions of area and velocity are given in Ref. 21.

If one accepts deviations between calculated and measured maximum forces of ±20%, these functions provide satisfactory force-time predictions of individual tests, as well as of averaged test data, for parachute experiments ranging from a 3-ft-diameter chute with 0.5-lb suspended load in wind-tunnel tests to a 100-ft-diameter chute with 5400-lb load in field tests. Values of the test conditions and the deviations of the maximum force values are given in Table 1.

In the course of this study, other pairs of functions were found which covered the same range of size, speed, and load. However, the accuracy of the force prediction based on these functions was slightly less than those of the so-called unique functions. All derived functions looked very similar to those shown in Fig. 9.

VI. Conclusion

In view of the agreement between measured and calculated data, the most interesting result is the fact that the time functions seem to represent the average time histories of the projected area and the net inflow velocity of solid flat circular parachutes at subsonic velocity.

Using the functions which approach uniqueness, the differences between the calculated maximum forces of several tests is, in general, less than the variation between the maximum forces of individual tests under identical test conditions. Therefore, maximum forces, calculated as shown here, may be considered to be indicative of averaged values of actual forces.

Acknowledgment

The study was sponsored by the U.S. Army Quartermaster Command, Natick, Mass., and the completion of the paper by the University of Minnesota.

References

[1] Mueller, W., "Fallschirme fuer Luftfahrzuege (Parachutes for Aircraft)," *Zeitschrift fuer Flugteknik und Motorluft-schiffahrt*, Heft No. 20, 1927.

[2] Weinig, F. S., *On the Dynamics of the Opening Shock of a Parachute*, USAF Office of Aeronautical Research, WADC, Dayton, Ohio, TR-6, Feb. 1951.

[3] Roberts, B. W., "Aerodynamic Inflation of Shell Type Parachute Structures," *Journal of Aircraft*, Vol. 11, July 1974, pp. 390-397.

[4] Payne, P. R., "A New Look at Parachute Opening Dynamics," *Aeronautical Journal*, Vol. 11, Feb. 1973, pp. 85-93.

[5] Wolf, D. F., "A Simplified Dynamic Model of Parachute Inflation," *Journal of Aircraft*, Vol. 11, Jan. 1974, pp. 28-33.

[6] McVey, D. F. and Wolf, D. F., "Analysis of Deployment and Inflation of Large Ribbon Parachutes," *Journal of Aircraft*, Vol. 11, Feb. 1974, pp. 96-103.

[7] O'Hara, F., "Notes on the Opening Behaviour and the Opening Forces of Parachutes," *Royal Aeronautical Society Journal*, Nov. 1949, pp. 1053-1062.

[8] Heinrich, H. G. and Bhateley, I. C., "A Simplified Analytical Method to Calculate Parachute Opening Time and Opening Shock," Summer Course on Aerodynamic Deceleration, University of Minnesota, July 1961.

[9] Heinrich, H. G., "A Linearized Theory of Parachute Opening Dynamics," *Royal Aeronautical Society Journal*, Vol. 76, Dec. 1972, pp. 723-730.

[10] Heinrich, H. G., "The Effective Porosity of Parachute Cloth," *Sonderdruck aus Zeitschrift fuer Flugwissenshaften* 11, Heft 10, Verlag Friedr, Vieweg and Sohn, Braunschweig, Germany, 1963.

[11] Von Karman, T., "Note on Analysis of the Opening Shock of Parachutes at Various Altitudes," U.S.-Army Aircorps Scientific Advisory Group, 1945.

[12] Heinrich, H. G., "Experimental Parameters in Parachute Opening Theory," *Bulletin of the 19th Symposium of Shock and Vibration*, Office of the Secretary of Defense, Washington, D. C., 1953.

[13] *Performance of and Design Criteria for Deployable Aerodynamic Decelerators*, U.S. Air Force Tech. Rept. ASD-TR-61-579, Dec. 1973.

[14] Heinrich, H. G. and Noreen, R. A., "Analysis of Parachute Opening Dynamics with Supporting Wind Tunnel Experiments," *Journal of Aircraft*, Vol. 7, July-Aug. 1970, pp. 341-347.

[15] Berndt, R. J., "Experimental Determination of Parameters for the Calculation of Parachute Filling Times," *Jahrbuch des Wissenschaftlichen Gesellschaft fuer Luft- and Raumfahrt, E. V. (WGLR)*, Friedr. Vieweg and Sohn Braunschweig, Germany, 1964, pp. 299-316.

[16] Uotila, J. I., "An Analysis of Parachute Opening Dynamics," Master of Science Thesis, University of Minnesota, Minneapolis, Minn., Aug. 1973.

[17] Unpublished data obtained from Air Force Flight Dynamics Laboratory Data Bank, Wright-Patterson AFB, Ohio, (J. H. DeWeese, Project Engineer).

[18] Ibrahim, S. K., "Apparent Added Mass and Moment of Inertia of Cup-Shaped Bodies in Unsteady Incompressible Flow," Ph.D. Thesis, University of Minnesota, Minneapolis, Minn., May 1965.

[19] Klimas, P. C., "Fluid Mass Associated with an Axisymmetric Parachute Canopy," *Journal of Aircraft*, Vol. 14, June 1977, pp. 577-580.

[20] Saari, D. P., "Dynamics and Stability of Lifting Parachutes," Ph.D. Thesis, University of Minnesota, Minneapolis, Minn., June 1976, p. 77.

[21] Heinrich, H. G., Noreen, R. A., and Saari, D. P., "A Parachute Opening Shock Theory Based on Non-Linear Time Histories of Inflow Velocity and Projected Area," U.S. Army Natick Labs. Tech. Rept. 75-10 AMEL, May 1974.